

New Laboratory Technique Measures Projected Dynamic Area of Prosthetic Heart Valves

Lawrence N. Scotten, David K. Walker

ViVitro Systems Inc., Victoria, Canada

Background and aim of the study: Fluid dynamic forces, valve design factors and gravity interactively determine the complex motion of prosthetic heart valve occluders. Although motion has been investigated, *in vitro*, using high-speed image recording, the technique has significant cost and limitations on resolution.

Methods: The kinematics of mechanical and biological valve occluders in the aortic and mitral positions were assessed by measuring projected dynamic valve area (PDVA). Valves were tested in a pulse duplicator system simulating normal cardiac conditions. To quantify PDVA, light passage through back-illuminated valves was measured by a calibrated photo-sensor with high-frequency response up to 150 kHz. Ten consecutive cycles were sampled using a PC data acquisition system. The system was calibrated under static conditions using reference areas.

Results: Several characteristics can be obtained from

The complex motion of prosthetic heart valves is governed by fluid dynamic and gravitational forces interacting with valve components. Valve dynamics vary greatly throughout the cardiac cycle, with occluder motion being most rapid during valve opening, closure and rebound. In the open phase, random oscillatory occluder motion can occur (1-4). Feldman et al. observed oscillatory mechanical valve behavior by using echocardiography (5). During closure, biological valves demonstrate more gentle closure than mechanical valves. At closure, mechanical valves rebound (6,7). Cavitation has been linked to rebound and fluid stress factors (6). In the closed state, mechanical valves normally exhibit a small amount of leakage that can

PDVA measurement including: maximum and minimum PDVA; rate of change of valve opening and closing PDVA; occluder rebound; and oscillatory open occluder behavior. Biological valves open more rapidly, close more gently, and exhibit no occluder rebound. They are also unaffected by gravity, and vary little in behavior from cycle to cycle compared with mechanical valves.

Conclusion: A new method for measuring PDVA has been developed. Distinct differences in performance between valves were identified. It is hypothesized that, aside from patient factors and differences in materials, mechanical valves that mimic the PDVA behavior of biological valves, will lead to reduction of thrombogenicity, cavitation and high-intensity transient signals (HITS), and also reduce sound level and regurgitation.

The Journal of Heart Valve Disease 2004;13:120-133

cause subclinical damage to blood elements (8).

Various imaging techniques have been used to record valve dynamics. In order to record images of high-speed events, a sufficient framing rate is required (see Appendix A), and rates ranging from 30 to 1000 frames per second have been used (9-20).

For mitral valves, Guo et al. developed a technique that used laser sweeping to measure occluder dynamics within the last 3° of closure (21). Testing of biological valves was not possible using this technique, and monitoring of valves at the aortic site would be problematic.

Herein, a new technique is described which quantified projected dynamic valve area (PDVA) over the entire cardiac cycle for mechanical and biological valves sited in either the aortic or mitral position.

Materials and methods

Pulse duplicator

A commercial pulse duplicator system (ViVitro

Presented at the Second Biennial Meeting of the Society for Heart Valve Disease, 28th June-1st July, Palais des Congres, Paris, France

Address for correspondence:

L. N. Scotten, ViVitro Systems Inc., 2400 Arbutus Road, Victoria, B.C., Canada V8N 1V7

e-mail: vivitro@horizon.bc.ca

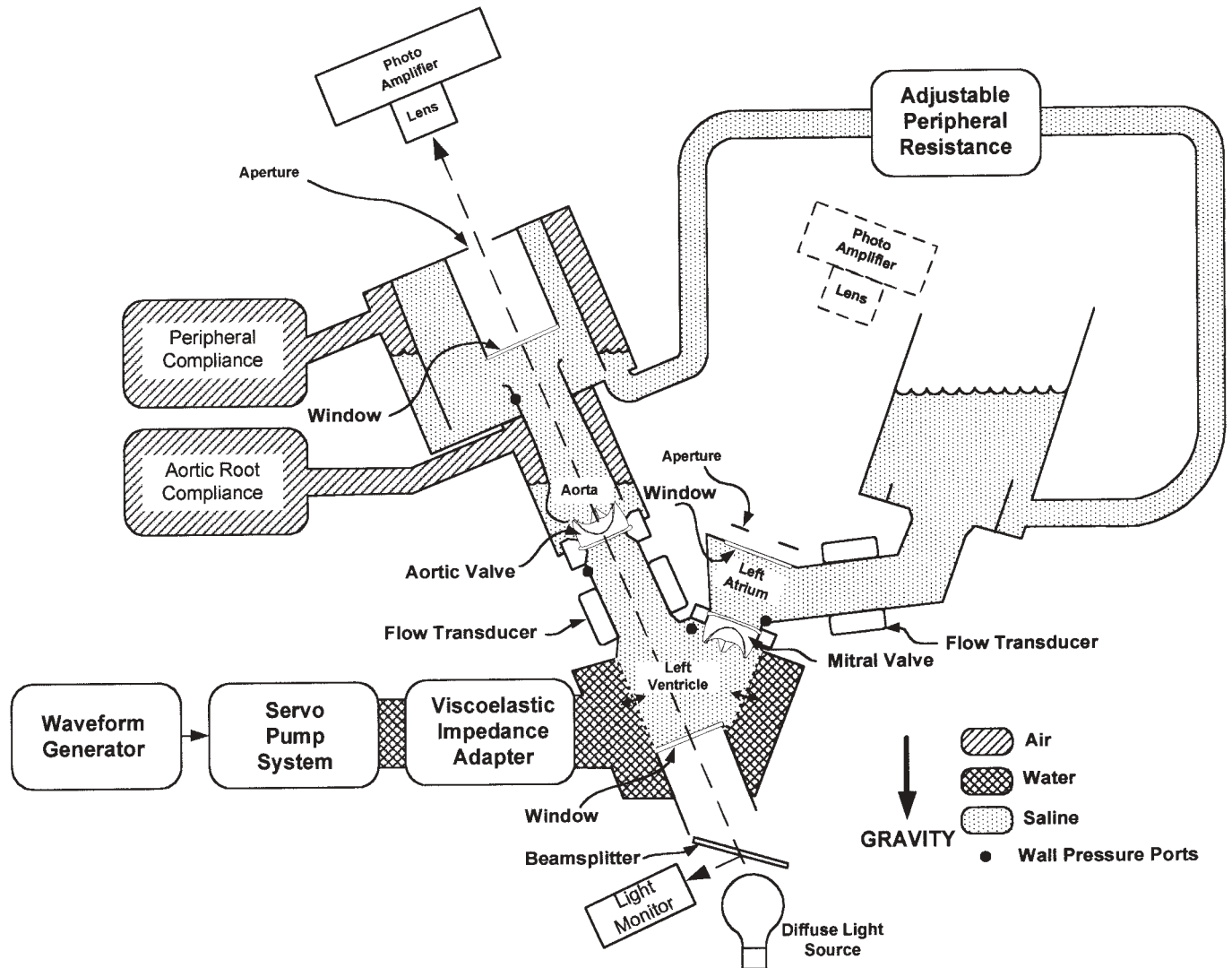


Figure 1: Commercial pulse duplicator and prototype photo-detection system for monitoring projected dynamic valve area (PDVA) at the aortic site. For mitral valve testing, the photo-detector and lens assembly is repositioned on the mitral valve axis and an alternative window alignment is used in the apex of the ventricle for light source transmission through the mitral valve. The direction of gravity is shown.

Systems, Inc.; Fig. 1), parts of which have been described previously (22), was used in the study. Valves were custom-mounted in compliant RTV silicone rubber seals (Silicones, Inc., GI-1100, with specified Shore A hardness of 22 ± 4). Valve orientation corresponded to a standing patient with gravity acting downwards, and occluder orientation with respect to aortic and mitral site structures was standardized.

It is recognized that viscosity can influence occluder kinematics, but in this initial study, blood viscosity was not modeled. Saline with density 1.0 g/ml and viscosity 1 mPas was used as a test fluid. The test conditions included: heart rate 70 beats/min; systolic/diastolic pressures $\sim 120/80$ mmHg; and cardiac output 5 l/min.

Photo-detection system and calibration

To quantify PDVA, light passage through back-illuminated valves was measured using a calibrated photo-detector. Experiments and calibrations were performed in a darkened room.

A PHLOX model #BL00204-00180 provided diffuse red light. Specified light source uniformity was $>90\%$ (5.08 cm square planar surface) and average luminance 840 cd/m^2 . A Burr-Brown (model OPT211P) photo detector was used. The sensor element was 2.29 mm square and placed 18 mm from the threaded base of a lens (CCTV, 16 mm, F1.6, Marshall #V-4516). A matte plastic screen and magnifying lens was positioned temporarily at the photo-sensor site to visually assist system alignment and focus. Apertures were used to

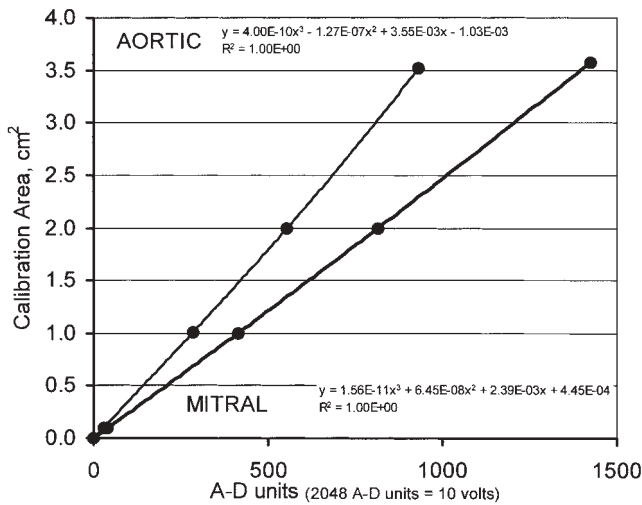


Figure 2: Calibration curves for photo-detector system. The Y- intercept is set to zero.

mask extraneous peripheral light coming from the test valve sites. The distance between the photo-sensor and the mid-plane of the test valve was ~37 cm in both aortic and mitral sites. A monolithic light-to-voltage optical sensor (Texas Instruments, TSL250) was used to monitor light source intensity.

Calibration assumed similar optical properties of the

static and dynamic test fluid. Test fluid clarity and biofilm contamination of window surfaces affected calibration, and care was taken to minimize their adverse influence.

Four reference orifices were used for calibration under static conditions. Orifices and test valves could be mounted with repeatable registration. Typical calibrations are shown in Figure 2, with third-order polynomial equations indicated. Calibration stability varied <0.2% over a one-day period; uniformity of calibration over valve test site region was >94%; and depth-of-field effects over a 12-mm range showed calibration variation <2%.

Test valves

The valves used in the study are listed in Table I. The biological valves included three bovine pericardial valves and one porcine valve, while the mechanical valves included two single disc and four bileaflet valves. All valves had a nominal tissue annulus diameter of 25 mm.

In order to evaluate system performance, this preliminary study compared valve performance in each site using the same valve. This was carried out even though some valves were specified for aortic use only. The M1 valve was specified for clinical use only at the aortic site.

Table I: Details of biological (B) and mechanical (M) valves tested.

Valve	Code	Type	TAD (mm)	FOA (cm ²)	EOA(cm ²)	
					Aortic	Mitral
Edwards (Perimount Model 2700)	B1	Pericardial	25	-	3.0	1.8
Edwards (Perimount Model 2800)	B2	Pericardial	25	-	2.9	1.6
CarboMedics (Mitroflow Synergy PC)	B3	Pericardial	25	-	3.0	2.0
CarboMedics (Labcor Synergy ST)	B4	Porcine	25	-	1.9	1.4
Medtronic-Hall (Aortic specification)	M1	Single disc	25	1.8	2.3	2.1
Omniscience	M2	Single disc	25	2.2	2.6	2.0
St. Jude Medical, Hemodynamic Plus (HP)	M3	Bileaflet	25	2.9	3.7	2.7
St. Jude Medical, Regent™ (SHP)	M4	Bileaflet	25	3.0	4.0	3.0
CarboMedics (SC Orbis, Model 200)	M5	Bileaflet	25	2.3	2.3	2.2
MCRI (On-X)	M6	Bileaflet	25	3.4	3.7	2.3

EOA: Effective orifice area (mean EOA_{_{cp}} and EOA were obtained from hydrodynamic measurements at the aortic and mitral sites over 10 consecutive cycles; see Appendix B).

FOA: Full open area (the projected FOA was measured by the photo-detector under static conditions. For compliant biological valves, FOA was not defined).

TAD: Tissue annulus diameter (manufacturer-specified).

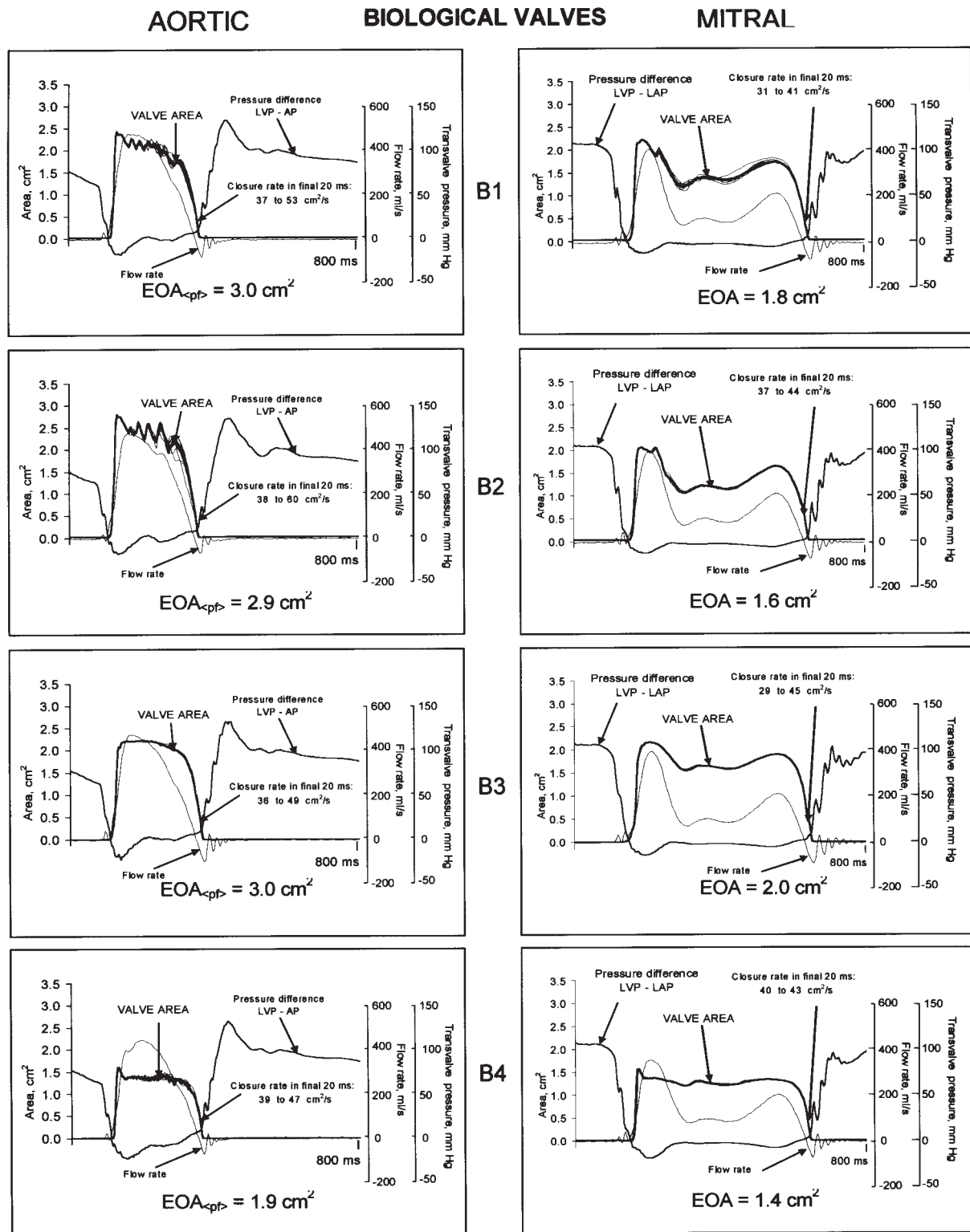


Figure 3: Projected dynamic valve area (PDVA) for biological valves in the aortic (left) and mitral (right) positions for each of 10 consecutive cycles (thin lines) and average (thick line). The PDVA closure rate range during the final 20 ms of closure is indicated for each valve and site. Average waveforms of 10 cycles are shown for volumetric flow rate and transvalve pressure waveforms (LVP - AP: Left ventricle pressure minus aortic pressure; LVP - LAP: Left ventricle pressure minus left atrial pressure). EOA_{pf} and EOA are hydrodynamic effective orifice areas (see Appendix B). Approximately one period of data is presented. Cycle rate 70 beats/min; cardiac output 5 l/min; test fluid is saline. Pressure and flow signal electronic filters are 100 Hz low pass. See Table I for valve legend.

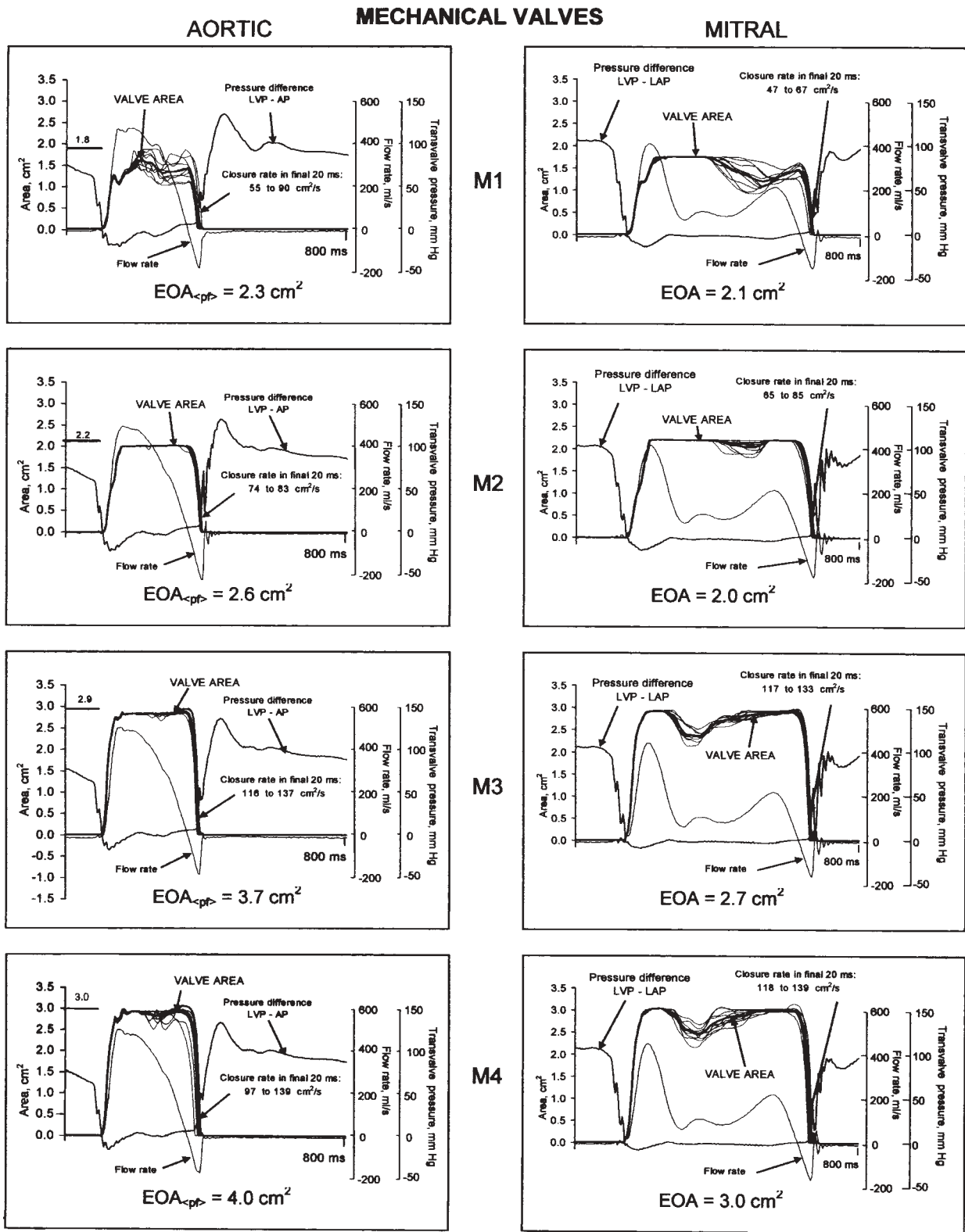


Figure 4: Projected dynamic valve area (PDVA) for mechanical valves in the aortic (left) and mitral (right) positions. On the aortic valve area axes, projected full open area limits (FOA) are indicated by a horizontal line. (See legend of Fig. 3 for further details.)

Figure continues on next page

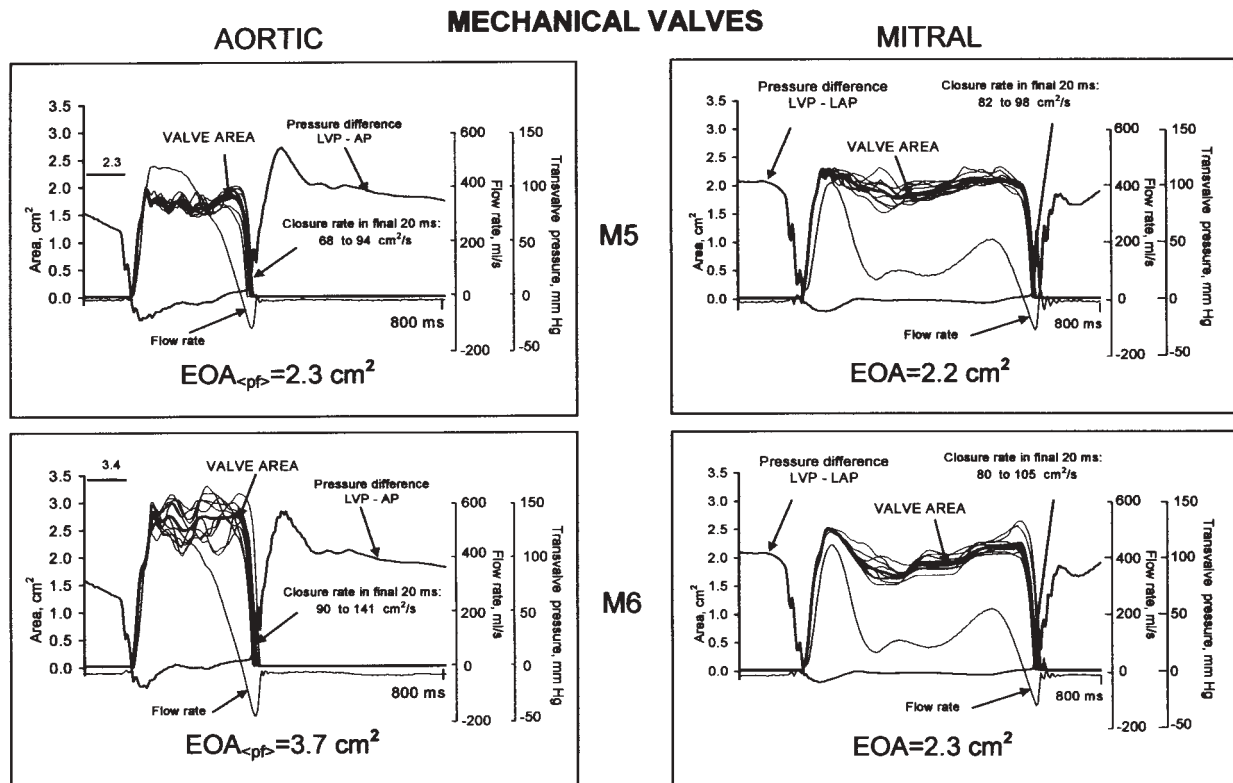


Figure 4 continued

Projected full open area

Mechanical valve occluder(s) were temporarily tethered open by a small suture line and mounted into the static fluid-filled model. Photo-detector measurements of projected full open area (FOA) limit are listed in Table I (see also Fig. 4). The suture line blockage of light was $<0.01 \text{ cm}^2$. Due to the highly compliant nature of biological valve leaflets, FOA cannot be specified with certainty for these devices and was therefore not included in Table I.

Data acquisition systems and analysis

A PC-based analog-to-digital board and a 100 MHz digital real-time oscilloscope (Tektronix TDS2014) were used for data acquisition. The acquisition sampling rate was 300 Hz using the A-D board, and 10 consecutive cycles were recorded for each valve tested. The oscilloscope was used to sample randomly the rapid rebound signals at 100 kHz. Software including VIVITEST^{VSI}, Microsoft EXCELTM and VISIOTM were used for data acquisition, analysis, display and plotting of results.

Oscillation frequencies in the PDVA signal during the valve open phase were determined by measurement of oscillations that could be clearly recognized as periodic in form. The average area closure rate was determined during the 20 ms period before closure.

Although measurement of valve hydrodynamics was obtained concomitantly with PDVA, in this report, primary emphasis was given to light-determined PDVA measurements.

Results

PDVA was measured over the entire cardiac cycle, and is shown in Figures 3 and 4 in conjunction with transvalve pressure and flow waveforms. Results over various phases in the simulated cycle are presented under the following headings.

Opening

PDVA and rate of change of PDVA (derivative with respect to time) during the initial 120 ms of the valve opening phase are shown in Figure 5. Derivative function emphasizes points of inflexion in PDVA. Valve opening motion was notably consistent from cycle to cycle, perhaps due to the stable nature of accelerating flow (23). The opening behavior was similar at each test site, despite differences in gravitational influence, pulsatile flow character and chamber geometry. This was particularly apparent for the biological valves, which are relatively unaffected by gravity. The biological valves opened more rapidly than the mechanical valves at both test sites. A single derivative peak was

characteristic for the biological valves, whereas multiple peaks occurred with the mechanical valves. For the mechanical valves, it appeared that the occluder pivot mechanisms closely steered occluder motion through distinct stages which engendered opening behavior unique to each valve.

Normal opening behavior of mechanical valves has been studied non-invasively (24,25), with the performance of Medtronic-Hall valves being evaluated in a series of 15 patients. Three characteristic opening clicks (OC₁, OC₂, OC₃) were recorded using phonocardiography, and correlated with features in M-mode echocardiography. A characteristic tri-phasic sliding disc motion during the opening phase was suggested as the cause of the clicks. The three clicks were reported to be: OC₁ to OC₂ = 31.2 ± 7.7 ms and OC₂ to OC₃ = 32.3 ± 7.5 ms. Comparable *dA/dt* inflexion point timings are shown in Figure 5. Here, the intervals for mitral and [aortic] valves were: OC₁ to OC₂ = 32.9 ms [29.0 ms] and OC₂ to OC₃ = 37.0 ms [35.5 ms]. These results appear to support the test system simulation at both the mitral and aortic sites (22) for this valve.

Open

Evaluation of normally functioning prosthetic valves in various settings has shown that leaflet flutter can occur, and the valves may not open fully (2,5,18). In the present study, some valves exhibited oscillations during the open valve phase (see Figs. 3 and 4; data listed in Table II). The range of frequency measured in the present study supports some predictions (4) and in-vivo observations (5). At the aortic site, the B4 porcine valve had a low flutter amplitude and the highest flutter frequency of ~150 Hz. The B3 and M2 valves had

Table II: Specific frequency or frequencies and respective period or periods (n, n) associated with projected dynamic valve area (PDVA) flutter exhibited over forward-flow phase at aortic and/or mitral sites.

Valve	Frequency (Hz)	Period (ms)
B1	30, 46	33, 22
B2	30, 46	33, 22
B3	None	None
B4	150	7
M1	31	32
M2	None	None
M3	50	20
M4	30	33
M5	22, 52	45, 19
M6	13, 28	77, 36

Cycle rate 70 beats/min; cardiac output 5 l/min; test fluid is saline. Samples were obtained from the average of 10 waveforms. Flutter was negligible in valves B3 and M2

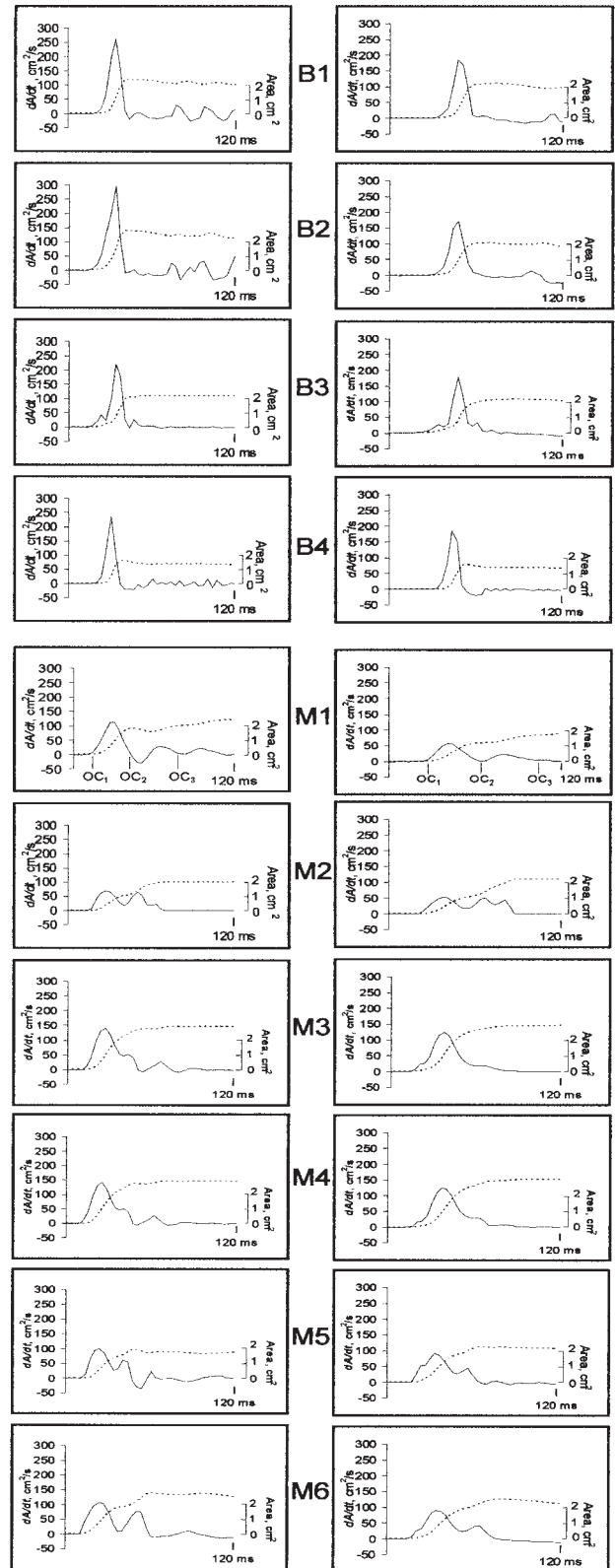


Figure 5: Aortic and mitral valve PDVA (dashed lines) and derivative, *dA/dt*, (solid lines) over a duration of 120 ms at the initial valve opening. Cycle rate 70 beats/min; cardiac output 5 l/min. Test fluid is saline. See Table I for valve legend.

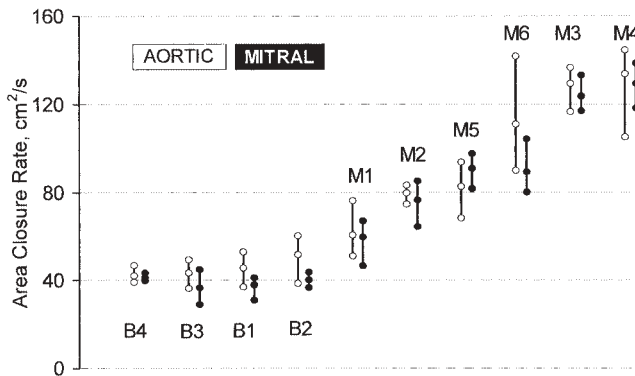


Figure 6: Range (upper and lower data point) and mean (central data point) of aortic and mitral valve PDVA closure rate (cm^2/s) averaged from the data sampled during the final 20 ms of closure over 10 consecutive cycles for biological and mechanical valves. Cycle rate 70 beats/min; cardiac output 5 l/min; test fluid is saline. See Table I for valve legend.

negligible flutter at either test site.

Maximum PDVA ranged from 1.6 cm^2 for the B4 valve to the largest open PDVA of 3.0 cm^2 for the M4 valve. The M1 valve, when at the aortic site, demonstrated variable, cycle-dependent open PDVA after the initial opening phase (Fig. 4). This can be seen from the large range of open PDVA over the 10 consecutive cycles. In vivo, the M1 aortic valve demonstrated incomplete opening of $60\text{--}65^\circ$, rather than the maximum possible of 75° for the aortic valve (26). The maximum aortic valve PDVA for the M1 valve, averaged over 10 cycles, was 7% less than FOA (1.6 cm^2 rather than 1.8 cm^2) (Fig. 4).

In Figure 4, the M2 valve is shown to be 6% less than fully open (PDVA = 2.1 cm^2 rather than 2.2 cm^2) at the aortic site but, when assisted by gravity and/or flow forces, was fully open at the mitral site. In one report (27), the M2 valve was imaged in vivo and found to open to less than 50° (maximum possible 80°). On average, the M3 valve at the aortic and mitral sites opened to a maximum PDVA of 2.8 cm^2 , which was about 5% less than FOA (2.9 cm^2). Likewise, the M5 valve opened to 2.0 cm^2 , about 13% short of the FOA limit of 2.3 cm^2 . The M6 valves opened to 2.9 cm^2 , 14% less than the FOA of 3.4 cm^2 .

The biological valves opened to the same maximum PDVA from cycle to cycle, and were negligibly influenced by gravity (Fig. 3). At the end of the opening phase, the B1 and B2 pericardial valves had a brief maximum PDVA of 2.5 cm^2 and 2.8 cm^2 at the aortic and mitral sites, respectively. The B3 pericardial valve exhibited little flutter and a maximum PDVA of 2.3 cm^2 . The porcine valve B4 had the least maximum PDVA of all valves ($\sim 1.6 \text{ cm}^2$).

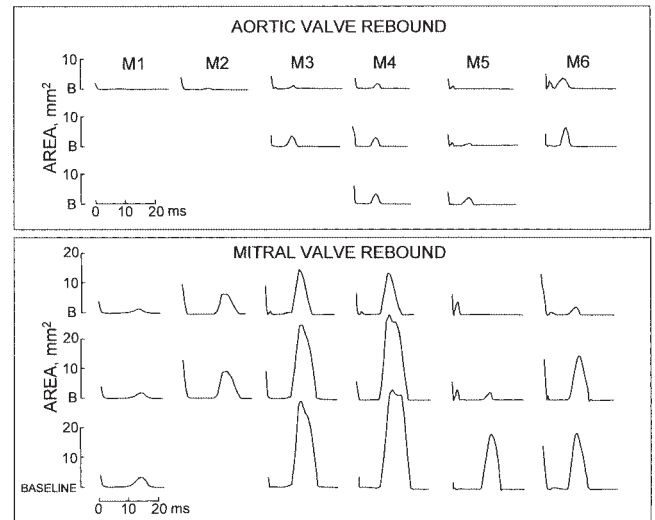


Figure 7: Random sampling of mechanical valve rebound waveforms at the aortic and mitral sites. Up to three samples are shown for each valve and site, with number of samples indicative of propensity for waveform variation from cycle to cycle. Baseline (B) is the closed valve area. Cycle rate 70 beats/min; cardiac output 5 l/min; test fluid is saline. See Table I for valve legend.

Closing

Relative to the zero flow state at the end of forward flow, results indicate that the biological valves close sooner than the mechanical valves. As a result, measured closing regurgitation of the biological valves was somewhat less than for the mechanical valves. PDVA closure rate indicated that the biological valves closed more gently than the mechanical valves.

During the final 20 ms of closure, mean PDVA closure rate range over 10 cycles for each valve, cycle and test site is shown in Figures 3, 4 and 6. For both valve sites, it should be noted that the magnitude of valve differential pressure drives the valve closure rate - not the rate of change of valve differential pressure. Closure rate was somewhat greater at the aortic site than at the mitral site. This correlates to a greater differential pressure at the aortic site than at the mitral site just prior to closure. For example, at the aortic site, the mean differential pressure for M6 in the final 20 ms prior to valve closure in one cycle was 10 mmHg versus 4 mmHg at the mitral site.

Mitral valves have usually been investigated with regard to cavitation (28-30). The reported rationale for using mitral valves for such investigations was given as: (i) low pressure is critical to cavitation, and pressure is usually minimal on the left atrial side of mitral valves; and (ii) valve closure rate is greatest for mitral valves which are closed by a high left ventricle pressure. The present results indicate that mechanical valves at the aortic site have somewhat higher PDVA

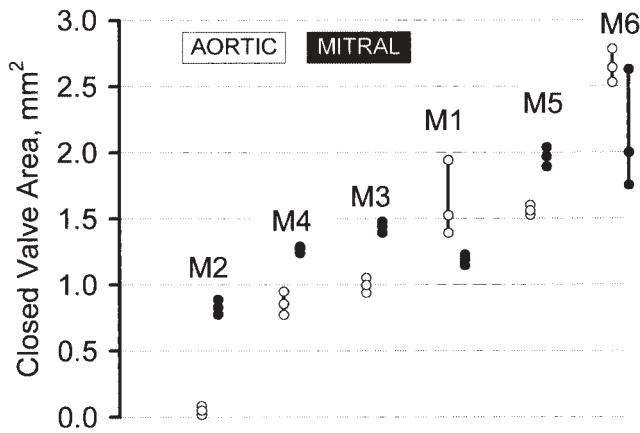


Figure 8: Closed valve PDVA (mm²) over 10 consecutive cycles for mechanical valves at the aortic and mitral sites.

closure rates because of greater valve differential pressure prior to closure. For this reason, aortic valves may be more prone to cavitation and/or high-intensity transient signals (HITS) than valves at the mitral site, although simulation of other physiological conditions may affect this finding.

Rebound

Mechanical valve occluders have high kinetic energy at closure which is dissipated, in part, by occluder rebound. Random samples of valve rebound were chosen for illustration (Fig. 7). The number of samples displayed is indicative of the propensity for variation in rebound behavior from cycle to cycle over approximately 300 visually observed cycles.

Typically, the amplitude and duration of mitral valve rebound was greater than for aortic valves. This may be partially due to gravity tending to re-open mitral valves and reinforcing aortic valve closure. In one study (31), an increase in mitral suturing ring compliance increased valve rebound time and decreased closing impact force. In other reports (32,33), an increase in mitral valve mounting compliance elevated cavitation threshold with respect to left ventricular pressure slope (dp/dt). In the present study, differences in aortic versus mitral rebound behavior were not likely related to valve mounting compliance since, for a given valve, the same rubber seal was used and a similar clamping force applied at each site. The bileaflet valves (M3-M6) usually had greater rebound amplitude and cycle-to-cycle variation than the single-disc valves (M1 and M2). Multiple rebound behavior occurred occasionally, but only with the bileaflet valves. Valve rebound was very small with the M1 valve. No rebound occurred with the biological valves.

Closed

PDVA during the closed valve phase is shown in

Figure 8. Pivot zone leakage area and the closed area of biological valves are not properly accounted for using the photo-detector technique. For the M1 valve, pivot obstruction of light would cause for a larger percentage error in reported closed area than in the open area. Unlike the other mechanical valves, valve M2 seat design allows for occluder overlap - a feature which prevented the passage of light when this valve was closed. For this reason, M2 exhibited the least closed PDVA particularly in the aortic site where system light sensitivity was less than in the mitral site. It was not equal to zero because in this initial investigation, system calibration did not associate zero PDVA with residual ambient light. This may also be a reason for the difference, for a given valve, in measured closed valve PDVA between the aortic and mitral sites.

For a given valve, a small but measurable variance of closed valve PDVA occurred from cycle to cycle. This suggests that occluder seating varied with each cycle and was likely due to the typical free fit tolerances of mechanical valves.

Discussion

Unlike biological valves, implanted mechanical valves typically require lifelong anticoagulation and exhibit HITS. The disparities between mechanical and biological valve types remain manifest, and the reasons for them unresolved.

Using transcranial Doppler ultrasound, emboli in the bloodstream of patients with mechanical valves are evidenced by HITS - these are probably small gaseous bubbles in the bloodstream (34-36). Such emboli, it is reported, could be a cause of patient morbidity and mortality, although evidence for this remains controversial. Deklunder et al. (34) have reported an alteration of cognitive abilities in patients with mechanical heart valves. The full clinical implications of HITS remain a concern according to Milo et al. (35), though in contrast Nadareishvili et al. (36) found "a lack of association between HITS, clinical symptoms and cognitive functioning suggesting harmless epiphenomena".

Potentially relevant differences between mechanical and biological valve PDVA behavior have been measured using this new laboratory technique. It was found that the mechanical valves did not maintain their maximum opening throughout systole or diastole, in contrast to the findings of other investigators (19,37). For example, the measured open behavior of the M1 valve in the present study was different to that stated by Akins (37) in which "Complete opening of the single disc of the Medtronic-Hall valve is virtually always achieved both in terms of rotation and translation and also in terms of maintenance of the open position" was

attributed. Discrepancies in reported valve motion may be due to the limited framing rate used for recording valve motion (see Appendix A) and/or differences in the influence of gravity. Evidence of gravitational influence has been observed clinically (5). Also, open area is affected by implant orientation relative to aorta boundaries and the force of gravity. Differences in test fluid viscosity may also have an influence. In other studies, mechanical valves have demonstrated unpredictable leaflet position during decelerating flow (13), and occluder motion was described to be "complex and somewhat random" (21).

The consequence - if any - of occluder flutter in the clinical setting, is uncertain, and either detrimental and/or beneficial effects may occur. Although occluder oscillations were evident in most of the valves tested (particularly at the aortic site), only minimal effect on valve pressure drop was measured. For example, the variation in range of mean pressure drops over 10 consecutive cycles for the M1 and M6 aortic valves was 1.2 and 1.5 mmHg, respectively. The range for the B3 and M2 aortic valves, which had negligible flutter, was <1 mmHg.

In a model study, Thubrikar et al. (15) recorded flutter in both intact and implanted porcine aortic valves within fresh natural porcine aortic roots. The results of their study indicated that aortic valve flutter may be normal even with unfixed natural aortic valves and the sinuses of Valsalva, which are included in the present model, may play a substantial role in aortic valve flutter behavior (16).

Damage to blood cells and valve materials has been linked to in-vivo cavitation (38). Valve closure can cause high fluid stresses and low pressures, and this may initiate cavitation and/or HITS. Squeeze flow, rarefaction waves and vortex flow are other phenomena caused by fluid-valve interaction which encourage cavitation, and these should be avoided. Valve mechanisms designed to deal efficiently with closure energy, such as early closure and slow closure rate, may have clinical benefits (14).

Further understanding of cavitation, HITS and acoustic emission is being pursued on many fronts, both in vitro and in vivo. Takiura et al. (39) recently reported a new in-vitro method to evaluate valve cavitation phenomena based on measuring faint light emissions (sonoluminescence). In-vitro efforts to correlate such phenomena to valve kinematics can now be aided by the method reported here.

The effective orifice area (EOA) for a valve was regarded by Shandas et al. (40) to be the cross-sectional area available for flow at the vena contracta. In their study, laser flow imaging techniques were used to measure jet core area at the vena contracta distal to St. Jude Medical (SJM) mechanical valves. The total area

of the jet core was considered to reflect the area available for flow. Information about this area, it was suggested, would help in validating hydraulic formulae and Doppler techniques commonly used in valve studies to estimate EOA.

PDVA data and EOA offer different area determinations associated with a valve. PDVA relates to projected valve boundaries, whereas EOA - as indicated by Shandas et al. (40) - seeks to convey information about total fluid jet core area.

PDVA data are obtained with reference to the optical axis of the test system. This may be approximately coincident with the flow direction for centrally opening valves such as biological valves, but would be less so for other valves such as mechanical valves. For a valve such as the Starr-Edwards, the optical path would be completely obstructed and both PDVA and FOA would be zero, yet the EOA would be quantifiable. For this extreme example, it is clear that EOA values would be greater than both the open phase PDVA value and the FOA.

In the present study, $EOA_{_{opt}}$ and EOA were calculated as explained in Appendix B. These areas have not been validated in the manner described by Shandas et al. (40), but are nonetheless listed in Table I as the aim was to make comparisons with the PDVA and FOA data.

When comparing test results for the 25 mm SJM valve (HP model), Shandas et al. (40) identified a total jet core area ranging between 2.8 and 3.0 cm² over the open phase in pulsatile flow at 70 beats per minute. In a previous aortic valve study on this valve (44), $EOA_{_{opt}}$ was 3.08 ± 0.09 cm² which is close to Shandas's finding. In the present study, the $EOA_{_{opt}}$ for this aortic valve was 3.7 ± 0.1 cm² which is greater than the present authors' previous findings. The reason(s) for the discrepancy between the current and prior results may relate to differences in simulated test conditions, but this awaits further investigation. Maximum PDVA and FOA results from the present study were both 2.9 cm² and correlated with the results of Shandas et al. (40).

In a previous study (22), if the geometric aortic valve area was >1.3 cm², the area was overestimated when the Gorlin equation was applied. In the present study, maximum PDVA values for the aortic valves ranged from 1.6 to 2.8 cm², and FOA from 1.8 to 3.4 cm². Therefore, $EOA_{_{opt}}$ predictions for aortic valves were expected to overestimate maximum PDVA values.

For most of the aortic and mitral valves tested, their respective maximum PDVA values were close to FOA values in some or all cycles, with the M6 mitral valve being the notable exception.

Study limitations and prospective considerations

The present study was limited to evaluating size 25

mm valves under simulated normal cardiac conditions. The model heart can be adjusted to simulate compromised cardiac conditions, including ventricular fibrillation, low cardiac output and pathophysiological systemic and ventricular compliance. Investigation of valve motion under these adverse states is pending. Such studies may help to distinguish cause from effect issues with regard to prosthetic valve function. Caution is therefore advised in extrapolating the results of this limited study to other valve sizes and different physiological states. Valve motion with test fluids of different viscosity and viscoelastic properties may also be important.

Potential adverse illumination components, such as reflected light from shiny valve surfaces, translucent light from biological valves, or residual room light may add to the PDVA signal at indeterminate times in the cycle. Reflected light artifact could possibly be reduced by using optical techniques involving parallel light and/or polarized light. Blue light would reduce translucent light through biological valves. Light source and photo-detector electronics can be modified to allow studies to be conducted in normally lighted room conditions. Likewise, an automatic control of light source intensity could be implemented.

PDVA does not relate directly with occluder velocity. Nevertheless, in relative terms a lower PDVA closure rate means a lower occluder velocity for valves of similar design. Impact velocity occurs at the moment of valve closure, and is a parameter used in cavitation studies (41). If the measurement of impact velocity is desired, then revised optics would be required. The occluder under investigation would be imaged onto a slit-type aperture aligned appropriately, and a second lens would be used to image this aperture onto the photo-detector. The detected signal would then be proportional to occluder edge linear velocity that could be transformed into angular velocity, knowing valve geometry.

Acoustic emissions from mechanical valves can be substantial, and patient quality of life issues are implicated with audible valve sounds (42). The correlation of valve sound with motion could help in developing valve specific techniques to detect normal and abnormal valve function (43), and in designing quieter valves (14).

Computational fluid dynamic (CFD) modeling of valve dynamics has been increasingly presented as a design tool for prosthetic valves, yet simulation models have not reported the range of valve kinematics as measured herein. PDVA measurement capability should facilitate the validation of simulation models.

Preliminary tests on biological valves have indicated that visually assessed valve function correlated with characteristic features within the PDVA signal. This

suggests that the new technique may find application in the quality control of prosthetic valves. Moreover, the system could also be adapted to assess devices such as stentless valves and percutaneous valves. The growth and function of tissue-engineered valves in bioreactors could also possibly be evaluated using the new technique.

The new technique described herein has a comparable high-speed imaging rate of 16,000 frames per second. By using higher frequency response photo-sensors, an equivalent imaging rate of one million frames per second is anticipated which, in combination with appropriate lighting schemes, would allow continuous monitoring of cavitation and/or HITS bubbles.

Acknowledgements

The authors thank the valve manufacturers for supplying the test valves used in these studies, and for their comments related to this investigation. Some valves were supplied for previously published studies that were unrelated to the data presented here.

References

1. Reif TH, Huffstutler MC, Jr. Design considerations for the Omniscience pivoting disk cardiac valve prosthesis. *Artif Organs* 1983;6:131-138
2. Cheon GJ, Chandran KB. Dynamic behavior analysis of mechanical monoleaflet heart valve prostheses in the opening phase. *J Biomech Eng* 1993;115:389-395
3. Prabhu AA, Hwang NHC. Dynamic analysis of flutter in disk type mechanical heart valve prostheses. *J Biomech* 1988;21:585-590
4. Reif TH, Schulte TJ, Hwang NH. Estimation of the rotational undamped natural frequency of bileaflet cardiac valve prostheses. *J Biomed Eng* 1990;112:327-332
5. Feldman HJ, Gray RJ, Chau A, et al. Noninvasive in vivo and in vitro study of the St. Jude mitral valve prosthesis. *Am J Cardiol* 1982;49:1101-1109
6. Kini V, Bachmann C, Fontaine A, et al. Flow visualization in mechanical heart valves: Occluder rebound and cavitation potential. *Ann Biomed Eng* 2000;28:431-441
7. Zapanta CM, Stinebring DR, Deutsch S, et al. Correlation of prosthetic heart valve cavitation and valve leaflet dynamics. *Ann Biomed Eng* 1996; 24(suppl.1):S-2
8. Steegers A, Paul R, Reul H, Rau G. Leakage flow at mechanical heart valve prostheses: Improved washout or increased blood damage? *J Heart Valve Dis* 1999;8:312-323
9. Scotten LN, Walker DK, Brownlee RT. Construction and evaluation of a hydro-mechanical simulation

- facility for the assessment of mitral valve prostheses. *J Med Eng Tech* 1979;3:11-18
10. Wieting DW, Kafesjian R, Stobie R, et al. Hi-speed videography of Edwards-Duromedics heart valve dynamics and fluid dynamics. *Artif Organs* 1990;13:608
 11. Barbaro V, Boccanera G, Daniele C, et al. In-vitro test comparison of prosthetic heart valve: Closing phase. *Artif Organs* 1993;16:469
 12. Naemura K, Ohta Y, Fujimoto T, et al. Comparison of the closing dynamics of mechanical prosthetic heart valves. *Am Soc Artif Intern Organs J* 1997;43:M401-M404
 13. Ohta Y, Okamoto K, Sonderegger M, et al. Nonsymmetric leaflet motion of St. Jude Medical mitral valves simulated with a computer-controlled hydraulic mock circulator. *Artif Organs* 1997;21:335-339
 14. Naemura K, Umezu M, Dohi T, et al. Preliminary study on the new self-closing mechanical mitral valve. *Artif Organs* 1999;23:869-875
 15. Thubrikar MJ, Konstantinov IE, Selim GA, et al. The influence of sizing on the dynamic function of the free-hand implanted porcine aortic homograft: An in vitro study. *J Heart Valve Dis* 1999;8:242-253
 16. Robicsek F, Thubrikar MJ. Role of sinus wall compliance in aortic leaflet function. *Am J Cardiol* 1999;84:944-946
 17. Ohta Y, Kikuta Y, Shimooka T, et al. Effect of the sinus of Valsalva on the closing motion of bileaflet prosthetic heart valves. *Artif Organs* 2000;4:309-312
 18. Feng Z, Nakamura T, Fujimoto T, et al. In vitro investigation of opening behavior and hydrodynamics of bileaflet valves in the mitral position. *Artif Organs* 2002;26:32-39
 19. Shipkowitz T, Ambrus J, Kurk J, et al. Evaluation technique for bileaflet mechanical valves. *J Heart Valve Dis* 2002;11:275-282
 20. D'Souza SS, Butterfield M, Fisher J. Kinematics of synthetic flexible leaflet heart valves during accelerated testing. *J Heart Valve Dis* 2003;12:110-120
 21. Guo GX, Xu CC, Hwang NHC. Laser assessment of leaflet closing motion in prosthetic heart valves. *J Biomed Eng* 1990;12:477-481
 22. Scotten LN, Walker, DK, Dutton, JW. Modified Gorlin equation for the diagnosis of mixed aortic valve pathology. *J Heart Valve Dis* 2002;11:360-368
 23. Yoganathan AP, Cape EG, Sung H, et al. Review of hydrodynamic principles for the cardiologist: applications to the study of blood flow and jets by imaging techniques. *J Am Coll Cardiol* 1988;12:1344-1353
 24. Tabata T, Fukuda N, Iuchi A, et al. Clinical significance of the click intervals for the diagnosis of dysfunction of the Medtronic Hall prosthetic valve (in Japanese). *J Cardiol* 1992;22(suppl.IIV III):117-128
 25. Fukuda N, Oki T, Tabata T, et al. Comparative phonocardiographic, echocardiographic and Doppler echocardiographic evaluation of normally functioning Medtronic Hall and Björk-Shiley mitral prosthetic valves. *J Heart Valve Dis* 1994;3:275-282
 26. Ohta Y, Horiuchi T, Dohi T, et al. Development of computer aided motion analyzing (CAMA) system for radiopaque implanted tilting disc heart valves. *Artif Organs* 1990;14:449-453
 27. Edwards MS, Russell GB, Edwards AF, et al. Results of valve replacement with Omniscience mechanical prostheses. *Ann Thorac Surg* 2002;74:665-670
 28. Graf T, Fischer H, Reul H, et al. Cavitation potential of mechanical heart valve prostheses. *Int J Artif Org* 1991;14:169-174
 29. Dexter EU, Aluri S, Radcliffe RR, et al. In-vivo demonstration of cavitation potential of a mechanical heart valve. *Am Soc Artif Intern Organs J* 1999;45:436-441
 30. Bachmann C, Kini V, Deutsch S, et al. Mechanisms of cavitation and the formation of stable bubbles on the Björk-Shiley Monostrut prosthetic heart valve. *J Heart Valve Dis* 2002;11:105-113
 31. Chiang T, Guo GX, Hwang NHC, et al. The effect of suture ring compliance of a mechanical heart valve on the kinematic and acoustic characteristics observed during valve closure. *Int J Artif Org* 1992;15:545
 32. Guo GX, Adlparvar P, Howanec M, et al. Effect of structural compliance on cavitation threshold measurement of mechanical heart valves. *J Heart Valve Dis* 1994;3(suppl.I):S77-S84
 33. Wu ZJ, Gao BZ, Hwang NHC. Transient pressure at closing of a monoleaflet mechanical heart valve prosthesis: Mounting compliance effect. *J Heart Valve Dis* 1995;4:553-567
 34. Deklunder G, Roussel M, Lecroart JL, et al. Microemboli in cerebral circulation and alteration of cognitive abilities in patients with mechanical heart valves. *Stroke* 1998;29:1821-1826
 35. Milo S, Rambod E, Gutfinger C, et al. Mitral mechanical heart valves: In vitro studies of their closure, vortex and microbubble formation with possible medical implication. *Eur J Cardiothorac Surg* 2003;24:364-370
 36. Nadareishvili ZG, Beletsky V, Black SE, et al. Is cerebral microembolism in mechanical prosthetic heart valves clinically relevant? *J Neuroimaging* 2002;12:310-315
 37. Akins, CW. Results with mechanical cardiac valvular prostheses. *Ann Thorac Surg* 1995;60:1836-1844
 38. Kafesjian R, Howanec M, Ward GD, et al. Cavitation damage of pyrolytic carbon in mechanical heart valve. *J Heart Valve Dis* 1994;3:52-57

39. Takiura K, Chinzei T, Abe Y, et al. A new approach to detection of the cavitation on mechanical heart valves. *Am Soc Artif Intern Organs J* 2003;49:304-308
40. Shandas R, Kwon J, Valdes-Cruz L. A method for determining the reference effective flow areas for mechanical heart valve prostheses in vitro validation studies. *Circulation* 2000;101:1953-1959
41. Wu ZJ, Hwang NH. Asynchronous closure and leaflet impact velocity of bileaflet mechanical heart valves. *J Heart Valve Dis* 1995;4(suppl.1):S38-S49
42. Nygaard H, Johansen P, Riis C, et al. Assessment of perceived mechanical heart valve sound level in patients. *J Heart Valve Dis* 1999;8:655-661
43. Hasegawa J, Kobayashi K, Matsumoto H. Ultrasonic closing click of the prosthetic cardiac valve. *IEICE Trans Inf Syst* 1998;E81-D:1517-1521
44. Walker DK, Brendzel AM, Scotten LN. The new St. Jude Medical Regent™ mechanical heart valve: Laboratory measurements of hydrodynamic performance. *J Heart Valve Dis* 1999;8:687-696

Meeting discussion

DR. HELMUT REUL (Germany): Thank you for presenting this very interesting new technique. It is based on a high-speed camera, and these cost about \$10,000, but that might be a more economical way to measure valve opening. This fast closure might be also the reason for the cavitation potential of mechanical valves. The FDA and the ISO standard is currently that they have the parameter left ventricular dP/dt . Could your method replace this parameter and show the area decrease rate?

MR. LAWRENCE N. SCOTTEN (Victoria, British Columbia, Canada): Yes, I think that is possibly true. Measurement of valve motion was a very sensitive indicator of valve function. You might see a large motion occur in the kinematics of the valve, but you would barely see it happen with the hydrodynamics. So yes, I think it is a much more sensitive measure of looking at valve motion.

DR. AXEL HAUBOLD (USA): In your system characteristics you mentioned a stability of less than 0.2%. What do you mean by uniformity greater than 94%?

MR. SCOTTEN: Uniformity means that when you look at different areas in the region that the valve is operating, then is the calibration in the corner of the valve consistent with that in the center region? We were looking at sensitivity uniformity over the cross-sectional area of the valve under test.

DR. IAN VESELY (USA): This is very nice work. Some leaflets are translucent on the tissue valves. Do you have to set a zero point when the valve is closed? And, in the case of the Edwards valve, can you detect that little triangular opening when it is closed?

MR. SCOTTEN: We were using a red, backlight source - which is not the best color to use for tissue valves. A blue light is better as it doesn't transmit as well through tissue. We did not readjust to zero with the tissue valves. Only a minimum amount of light or signal came through, and we were happy with that. Detecting the translucent light passing through tissue valves is something we may improve on in the future.

DR. VESELY: Could you detect the little triangular gap when the valve is closed - or what are your thoughts on that point?

MR. SCOTTEN: I haven't noticed that yet when looking at the results, but perhaps I will look a little more carefully.

DR. JOHN FISHER (United Kingdom): In the early stages of mechanical valve opening and the late stages of mechanical valve closure, the flow path is not a straight line. Clearly, there is a lot of deviation around the leaflets, and the light path is not going to be a straight line either. How does the system adapt to that?

MR. SCOTTEN: Of course, the light is a straight line path. We are not looking at flow that may deviate around a tilted mechanical structure - we are trying to integrate the area around the valve in whatever complex shape that structure takes. We are also hoping that the light is stopped at the edge of the valves, at the edge of the occluder structure.

DR. FISHER: So just before closure, when the flow path is deviating around the leaflet, that flow area would not be detected in its true form because the light path is not a straight line?

MR. SCOTTEN: Yes.

DR. REUL: So, in other words, you measure only the projected light?

MR. SCOTTEN: That's correct.

MR. ANDY CAMPBELL (USA): You mentioned using this as a quality control methodology. Have you looked at multiple valves within the same model and size to look for variations?

MR. SCOTTEN: We have done this with the Mitroflow valve to a limited extent, and we were seeing visible characteristics that showed up in signal characteristics from the area. There was a correlation between what an operator saw and what the signal was picking up, so there may be some signatures here that could be useful.

Appendix A: Estimation of image framing rate for assessing valve motion

Standard video cameras have often been used to record valve behavior despite the limited framing rate of 30 frames per second. With this low framing rate, the observation of behavior >4 Hz or rise time <90 ms is precluded. Even with the highest framing rate of 1,000 frames per second, reported used for studying prosthetic valves, dynamic behavior with frequencies >88 Hz or rise time <4 ms would be overlooked.

For non-aliased portrayal of sinusoidal motion over one cycle, it would be desirable to acquire a minimum of nine recorded images. As a guide, a suitable minimum imaging rate for recording oscillatory motion of say 100 Hz, would therefore be $9 \times 100 = 900$ frames per second. For recording transient motion with nine images, a recommended minimal framing rate would be $9 \times 0.35 / Tr$, where rise time Tr is the time taken, in seconds, for a transient event to go from 10% to 90% of full amplitude. So, for an event with a rise time of 1 ms, such as occurs with a 25 mm size mechanical valve rebound, a framing rate >3,150 frames per second would be desirable. The system presented herein is comparable to a high-speed imaging rate of 16,000 frames per second, and has performance potential up to 150,000 frames per second.

Appendix B: Effective Orifice Areas $EOA_{\langle p \rangle}$ and $EOA_{\langle f \rangle}$ (cm^2)

$$EOA_{\langle p \rangle} = RMS_{\langle f \rangle} / (51.6 \sqrt{\Delta P_{\langle p \rangle}})$$

where $\Delta P_{\langle p \rangle}$ is the mean transaortic pressure difference in mmHg computed over the positive pressure interval, and $RMS_{\langle f \rangle}$ is the root mean square flow (in ml/s) computed over the forward-flow interval. This formula is analogous to that given in the FDA Replacement Heart Valve Guidance, except that we have measured ΔP over the positive-pressure interval $\langle p \rangle$ rather than the forward-flow interval. The $\langle p \rangle$ interval corresponds to that traditionally used in clinical catheter measurements, and gives a more conservative estimate of EOA than using the $\langle f \rangle$ interval, as $\Delta P_{\langle p \rangle}$ is generally greater than $\Delta P_{\langle f \rangle}$ for aortic valves (44).

For the mitral valves in this study, the standard equation recommended by the FDA Replacement Heart Valve Guidance was used:

$$EOA = RMS_{\langle f \rangle} / (51.6 \sqrt{\Delta P_{\langle f \rangle}})$$

Root Mean Square flow (ml/s)

$$RMS_{\langle f \rangle} = \sqrt{(\sum f_i^2 / n)}$$

where f_i is the instantaneous flow rate at the i^{th} point of the n points in the forward-flow summation interval.